Hysteretic thermal switching due to readout power heating in kinetic inductance detectors

Pieter de Visser*†§, Stafford Withington‡ and David Goldie‡
*Kavli Institute of NanoScience, Faculty of Applied Sciences, Delft University of Technology, Lorentzweg 1, 2628 CJ Delft, The Netherlands
†SRON National Institute for Space Research, Sorbonnelaan 2, 3584 CA Utrecht, The Netherlands
‡Cavendish Laboratory, Cambridge University, JJ Thomson Avenue, Cambridge CB3 0HE, United Kingdom
§Contact: p.j.devisser@tudelft.nl

***Abstract*—Kinetic Inductance Detectors (KIDs) consist of thin-film superconducting resonators. An incoming photon breaks Cooper pairs, and causes the surface impedance of the resonator to change. The resonant frequency shifts, and the absorption event is recorded by monitoring the change in microwave transmission amplitude and phase. In this paper, we show that the power deposited by the microwave readout signal can cause the temperature of the quasiparticles in the superconducting film to switch between well-defined states. Experimentally, the effect appears as a discontinuity in the resonance curve, but is actually a hysteretic switching between thermal states as the readout frequency is swept up and down. We present numerical simulations that predict, quite clearly, the existence of hysteretic switching in low T_c superconducting resonators. The switching occurs as a direct consequence of the relationship between the readout power absorbed by the resonator as a function of temperature, and the finite thermal impedance of the quasiparticle-phonon coupling. This work may lead to an improvement of the power handling in KIDs, which is the easiest way of noise reduction in these devices, and to a better understanding of electron-phonon coupling in superconductors.**

I. Introduction

Kinetic Inductance Detectors (KIDs) consist of thin-film superconducting resonators (<10GHz) on sapphire, quartz, or silicon substrates. An incoming infrared, optical, or x-ray photon breaks Cooper pairs, and causes the surface impedance of the resonator to change. The resonant frequency shifts, and the absorption event is recorded by monitoring the change in microwave transmission amplitude and phase [1].

One of the key issues in improving KIDs for detector purposes is decreasing the amount of noise. Using phase readout, excess noise was found, which scales inversely with the amount of applied microwave readout power [2], [3]. Therefore increasing the power handling of resonators is one of the topics of current research. At certain power resonators start to show nonlinear behaviour, which gives the power limit for linear detection. On the other hand, a lot of research has been done on nonlinear effects in resonators, showing that vortices, thermal instabilities due to local hot spots [4] and a power dependent surface impedance [5], [6] can also cause strong nonlinearities in the resonator response. This kind of research focuses usually on superconductors with a high critical temperature and a high resistivity. Since the nonlinearities are used for amplification and other purposes, easier operation at higher temperature is favourable. Thermal effects described in literature cause nonlinearities due to local spots where the superconductor is driven normal. Also quasiparticle heating was described, but neglected usually due to the relatively low heat resistances of high T_c superconductors [5], [7], which cannot set up a significant temperature gradient between the electron system and the phonon system.

In this paper we describe a nonlinear effect in superconducting resonators due to the temperature-dependent readout power dissipated in the resonator and the thermal resistance due to the limited electron-phonon coupling. We present simulations showing that these two processes together give rise to multiple temperature states of the quasiparticle system when solving the heat balance equation. These temperature states manifest themselves as switching, and hysteresis, in the resonance curve. The effect of bistability due to different solutions of the heat balance equation was described earlier [8], but in the context of local instabilities, switching around T_c. We note that other nonlinear effects can still be present in superconducting resonators, but the temperature state switching we describe here is likely to be dominate at low temperatures, and does not necessarily involve hot spots.

II. Theory

The microscopic picture of the electrodynamic response of a superconductor was developed by Mattis and Bardeen [9]. The complex conductivity $\sigma = \sigma_1 - i\sigma_2$ describes the response of both Cooper pairs and quasiparticles to an applied electric field. The surface impedance of a superconductor can be calculated from the complex conductivity. For arbitrary thicknesses t, the surface impedance Z_s in the dirty limit is given by [10]

$$Z_s = \sqrt{\frac{i\mu_0\omega}{\sigma}}\coth(\sqrt{i\omega\mu_0\sigma}t), \quad (1)$$

where ω is the free space angular frequency, μ_0 the permeability of free space and σ the complex conductivity.

A quarter wave resonator consists of a shorted piece of transmission line. The input impedance for a shorted

transmission line Z_{line} is given by

$$\begin{aligned} Z_{line} &= Z_0 \tanh \gamma l = Z_0 \tanh(\alpha + i\beta)l \\ &= Z_0 \tanh\left(\frac{\beta}{2Q_i} + i\beta\right) l, \end{aligned} \quad (2)$$

where Z_0 is the characteristic impedance of the line, γ the propagation constant of the line and l the length of the line. To calculate the impedance of a superconducting microstrip line we follow the analysis by Yassin and Withington [11]. We leave out the very details of the specific calculations. For an ideal line $\alpha = 0$, so that at resonance when $l = \lambda/4$ the input impedance $Z_{line} \to \infty$. For a non-ideal line, we can define an internal quality factor $Q_i = \frac{\beta}{2\alpha}$, describing the losses in the transmission line. The ideal line case corresponds to an infinite Q_i.

To couple electromagnetic energy into the resonator, a small gap is introduced between the open end of the quarterwave resonator and the feedline. The capacitance of this gap loads the resonator. The impedance looking into the capacitance becomes

$$Z_{in} = \frac{1}{i\omega C_g} + Z_0 \tanh \gamma l, \quad (3)$$

where C_g is the capacitance of the gap, and the second term is the input impedance of the transmission line, taken from Equation 2.

In the case of a parallel circuit, the coupler can be seen as a 3 port system. Port 1 and port 2 are the left and right side of the feedline, and port 3 is at the resonator waveguide just under the coupler. What is typically measured is the transmission from port 1 to port 2, given by the transmission function or forward scattering matrix element S_{21}, which is given by

$$S_{21} = \frac{2}{2 + Z_0/Z_{in}}, \quad (4)$$

where Z_0 is again the impedance of the feedline and Z_{in} the impedance looking into the coupling capacitor as given by Equation 3. S_{21} can also be written in terms of its amplitude $|S_{21}|$ and phase θ by $|S_{21}|e^{i\theta}$, and the power transmission is given by $|S_{21}|^2$. The quality factor of the resonator can be defined as $1/Q = 1/Q_c + 1/Q_i$, where Q_c is the coupling quality factor.

A. Power dissipation

Although the resonator is made of a superconducting material, it has a small resistance and therefore dissipates power. The internal quality factor Q_i is a measure for the resistive losses in the resonator, which should decrease exponentially with decreasing temperature. However measurements show that the internal quality factor always saturates at values around 10^6 at $T/T_c \approx 0.2$, which means an additional loss. The source of this loss can be excess quasiparticles or loss at the surface or in the dielectric, but is not exactly known [12], [13]. To make a realistic estimate of the dissipated power we take this saturation into account by modifying the internal quality factor in Equation 2 in the following way

$$\frac{1}{Q_i} = \frac{1}{Q_{i,MB}} + \frac{1}{Q_{sat}}, \quad (5)$$

TABLE I
PARAMETERS OF A SIMULATED MICROSTRIP RESONATOR.

Parameter	Symbol	Value
Strip length	l	4 mm
Strip width	w	3 μm
Film thickness	t	200 nm
Dielectric height	h	200 nm
Gap capacitance	C_g	5 fF
Relative permittivity of dielectric	ϵ_r	11
Feedline impedance	Z_0	20 Ω

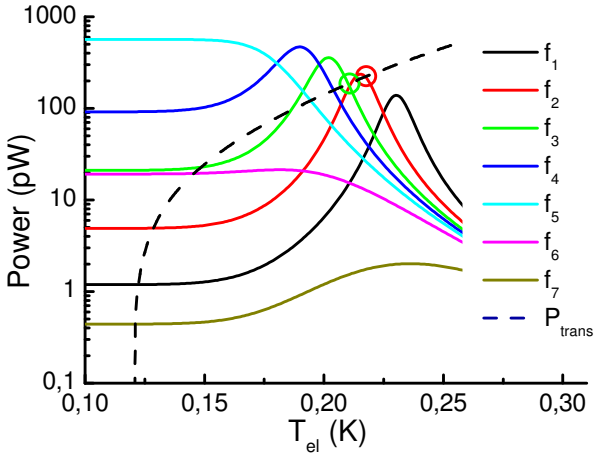

Fig. 1. Dissipated power in an Al microstripline resonator as a function of temperature for different readout frequencies. The readout power is -60 dBm. The dashed line shows the transported power due to electron-phonon coupling as a function of temperature according to $P_{trans} = -V\Sigma(T_e^5 - T_{ph}^5)$, for a phonon temperature of 120 mK.

where Q_{sat} is the saturation quality factor and $Q_{i,MB}$ the quality factor following the Mattis-Bardeen equations. In the calculations presented here we assume the additional loss to be due to quasiparticles. This is reasonable since we are interested in high readout power levels while dielectric losses saturate at a relatively low power level [13].

The dissipated power depends on how much power is coupled into the resonator, and therefore peaks at the resonance frequency. The resonance frequency is temperature dependent, and therefore the (peak in the) dissipated power is temperature dependent. Equally well we can define a resonance temperature for a particular frequency. The dissipated power is calculated for an Al microstrip resonator as a function of temperature and plotted in Figure 1 for different frequencies. The geometry properties are listed in Table I and material properties are $N_0V = 0.17$, T_D = 420 K and $\rho = 2.4$ $\mu\Omega$cm [14]. The readout power is 2 nW (-57 dBm) and the bath temperature 120 mK.

We observe that the resonance temperature is lower for higher frequencies as expected. At the highest frequencies a plateau is reached where the zero-temperature resonance frequency is approached and the saturation in the quality factor (Eq. 5) comes into play.

B. Heat transport

The resistance that causes the energy dissipation in the resonator is due to quasiparticles. When energy is dissipated into the quasiparticles, the quasiparticle system heats up and will transfer energy to the colder phonon system, and from the phonon system of the superconducting film to the phonon system of the substrate. The energy transport from electrons to phonons can be described for a metal by a power law [15]:

$$P_{e-ph} = V\Sigma(T_e^5 - T_{ph}^5), \quad (6)$$

where T_e is the electron temperature, T_{ph} the phonon temperature and V the volume where the power is dissipated. Σ is a material constant with a value of $\Sigma = 0.2 \times 10^9$ W m^{-3}K^{-5} for Al, measured in a Coulomb-blockade electrometer [16]. The volume can be calculated by $V = wtl$, where w and l are the width and length of the microstrip and t is the thickness of the film. For an Al microstripline with dimensions as given in Table I we get $V\Sigma$ = 480 nW K^{-5}. In Figure 1, the power transported by electron-phonon coupling as a function of temperature is plotted as the dashed line, for a phonon temperature of 120 mK.

In calculating the transported power, we assumed implicitly that electron-phonon coupling is the limiting heat transport mechanism. Another transport limiting heat resistance can be the Kapitza coupling between the film and the substrate of the resonator. The Kapitza coupling can also be described by a power law

$$P_{Kap} = A\Sigma_{Kap}(T^4 - T_{bath}^4), \quad (7)$$

where $A = wl$ is the area of the microstrip and Σ_{Kap} a material parameter. From Ref. [17] we estimate Σ_{Kap} to be 850 Wm^{-2}K^{-4} and $A\Sigma_{Kap}$ = 10 μWK^{-4} and therefore assume electron-phonon coupling being the limiting heat transport mechanism.

III. Simulations

Power is dissipated by the readout signal into the quasiparticle system of the superconducting film. This will increase the effective quasiparticle temperature. The phonon temperature of the film will be lower, so a temperature difference between the phonon- and electron system is set up, dependent on the strength of the electron-phonon coupling. From a steady state heat flow, the temperature of the electron system can be calculated by equating the dissipated power and the transported power. Finding the steady-state temperature for different readout frequencies and power levels is analogous to calculating the intersections of the dissipated power curve with the transported power curve in Figure 1. Steady state temperatures are calculated for every frequency using a root-finding algorithm which uses the steady state temperature of the previous frequency as an initial guess.

In Figure 2 the steady state temperature, and the resonator response of the same Al resonator, are plotted as a function of frequency for a set of readout powers. We observe that below 10 pW, the temperature rise is small and the resonance curve shows a deep symmetrical resonance. At 100 pW the electron temperature at resonance already rises 30 mK above the phonon temperature, making the resonance curve a bit less pronounced and introducing a frequency shift. Above 200 pW the resonance curve becomes asymetrical as a result of a 50 mK temperature rise and at 500 pW there is clear switching with hysteresis. For even higher powers, the operating temperature rises and the amount of hysteresis increases.

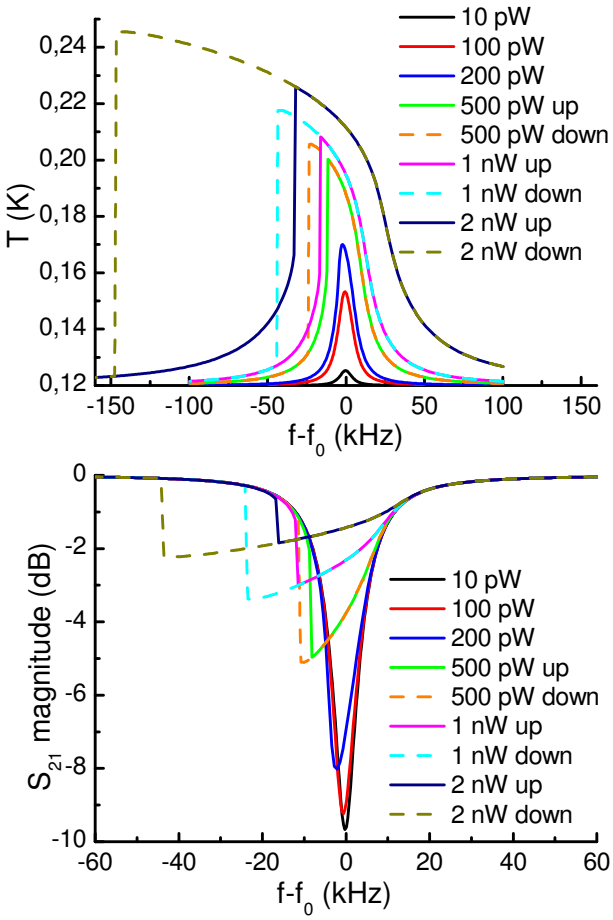

Fig. 2. Steady state temperature of the electron system (a) and the corresponding resonator response curve (b) for an Al microstripline resonator as a function of frequency for different readout power levels.

IV. Experiment

A 100 nm thick Al film was sputter deposited on a R-plane sapphire substrate under ultra high vacuum. The critical temperature of the film T_c is 1.228 K, the low temperature resistivity ρ was 0.63 $\mu\Omega$cm and the residual resistance ratio was 5.2 The resonator pattern was created using wet etching. A coplanar waveguide (CPW) resonator was used in the experiment, and therefore we can only make a qualitative comparison with the presented simulations. The chip was cooled in a cryostat with an adiabatic demagnetization refrigerator to a bath temperature of 81 mK. The complex transmission S_{21} of the chip was measured using a vector network analyzer.

The S_{21} magnitude is plotted as a function of frequency in Figure 3 for a set of readout power levels. For power levels below -81 dBm the response stays the same, except for

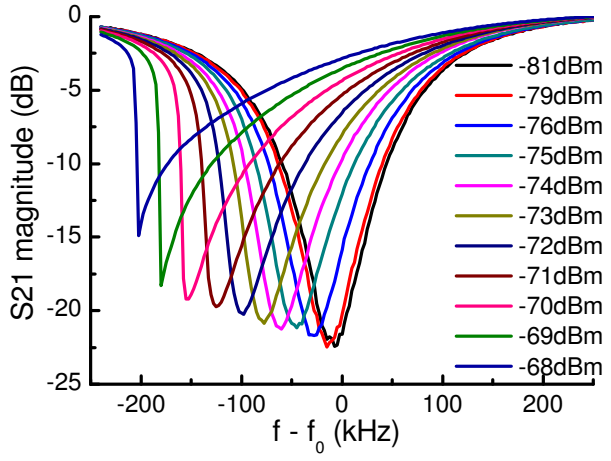

Fig. 3. Measured resonances curves of an Al coplanar waveguide resonator for different readout power levels. The bath temperature was 81 mK and f_0 = 4.55929 GHz.

the relative increase of noise. We observe that the resonance frequency decreases for increasing power, which is a sign of heating, because the resonance frequency shifts in the same way if the bath temperature is increased. Asymmetry in the resonance curve appears for a power of -75 dBm and true switching from -69 dBm, which is of the same order of magnitude as for the simulations in Figure 2.

V. Comparison on internal power

The most common way to compare the power handling of resonators is comparing them on internal power, which takes into account the quality factor dependent coupling of the readout signal to the resonator. The internal power, the power of the travelling wave inside the resonator, is given by

$$P_{internal} = P_{readout} \frac{2}{\pi} \frac{Q^2}{Q_c} \frac{Z_{feedline}}{Z_{resonator}}, \quad (8)$$

where $Z_{feedline}$ and $Z_{resonator}$ are the impedances of the feedline and the resonator. Using Equation 8 combined with the simulations presented in Section III we calculate an internal power of -22 dBm where the response becomes nonlinear. From the experimental data presented in Section IV we obtain a limiting internal power value of -30 dBm, which is a value commonly measured in Al KIDs of this thickness [18]. It is only possible to compare the internal power of devices just before the resonance curve becomes asymmetric since the quality factor cannot be obtained from a highly nonlinear resonance curve.

VI. Discussion

Experimental values for the limiting internal power before the resonator response becomes nonlinear are within an order of magnitude with the simulated values as presented above. This shows that thermal switching is a mechanism that is very likely to be present in resonators consisting of a low temperature superconducting film. However, there are other mechanisms that can be responsible for nonlinear behaviour. More detailed experiments are needed to explore the nonlinear effects that are observed experimentally in relation with the proposed thermal effect. Additional simulations are underway to compare the predictions about the limit to the internal power to experimental values with varying film thicknesses and film properties.

The assumed electron-phonon coupling is taken for a metal in the normal state and we believe that it could very well be an order of magnitude weaker for a superconductor, especially at temperatures much lower than T_c. This would bring the simulated power values where nonlinear behaviour starts remarkably close to the experimental data. We also implicitly assumed that the losses that determine the internal resonator quality factor are fully due to quasiparticles. Although there are also known dielectric losses, this assumption is better justified at higher readout powers, which is the regime we are operating in.

The two stable temperature states, with one unstable state in between, suggest that rapid switching between those three states can give excess noise. This could happen when the temperature difference between these states is small. Experiments show that as soon as the resonator is driven nonlinear, the noise increases quite significantly. However, more involved simulations and experiments are needed to investigate if the temperature states and the measured excess noise are correlated.

VII. Conclusion

We modelled the heat dissipation and heat transport in superconducting thin film resonators. We solved the heat balance, given by the temperature and frequency dependent microwave readout power dissipation together with limited electron-phonon transport described by a power law. For certain readout power levels this leads to multiple solutions to the steady state temperature giving hysteretic two state switching in the resonance curve. Simulated resonance curves as a function of power show qualitatively the same behaviour as experimentally observed resonance curves. With some refinements, the model could explain the microwave power handling in KIDs and could lead to an improvement of their performance.

References

[1] P. K. Day, H. G. LeDuc, B. A. Mazin, A. Vayonakis, and J. Zmuidzinas, "A broadband superconducting detector suitable for use in large arrays," *Nature*, vol. 425, p. 817, 2003.

[2] J. Gao, M. D. J. M. Martinis, A. Vayonakis, J. Zmuidzinas, B. Sadoulet, B. A. Mazin, P. K. Day, and H. G. Leduc, "A semiempirical model for two-level system noise in superconducting microresonators," *Appl. Phys. Lett.*, vol. 92, p. 212504, 2008.

[3] R. Barends, H. L. Hortensius, T. Zijlstra, J. J. A. Baselmans, S. J. C. Yates, J. R. Gao, and T. M. Klapwijk, "Noise in nbtin, al and ta superconducting resonators on silicon and sapphire substrates," *IEEE Trans. on Appl. Supercond.*, vol. 19, p. 936, 2009.

[4] B. Abdo, E. Sergev, O. Shtempluch, and E. Buks, "Escape rate of metastable states in a driven nbn superconducting microwave resonator," *J. Appl. Phys.*, vol. 101, p. 083909, 2007.

[5] C. C. Chin, D. E. Oates, G. Dresselhaus, and M. S. Dresselhaus, "Nonlinear electrodynamics of superconducting nbn and nb thin films at microwave frequencies," *Phys. Rev. B*, vol. 45, p. 4788, 1992.

[6] M. A. Golosovsky, H. J. Snortland, and M. R. Beasley, "Nonlinear microwave properties of superconducting nb microstrip resonators," *Phys. Rev. B*, vol. 51, p. 6462, 1995.

[7] P. Lahl and R. Wördenweber, "Fundamental microwave-power-limiting mechanism of epitaxial high-temperature superconducting thin-film devices," *J. Appl. Phys.*, vol. 97, p. 113911, 1995.

[8] A. Gurevich and R. Mints, "Self-heating in normal metals and superconductors," *Rev. Mod. Phys.*, vol. 59, p. 941, 1987.

[9] D. C. Mattis and J. Bardeen, "Theory of the anomalous skin effect in normal and superconducting metals," *Phys. Rev.*, vol. 111, p. 412, 1958.

[10] R. L. Kautz, "Picosecond pulses on superconducting striplines," *J. Appl. Phys.*, vol. 49, p. 308, 1978.

[11] G. Yassin and S. Withington, "Electromagnetic models for superconducting millimetre-wave and sub-millimetre-wave microstrip transmission lines," *J. Phys. D. Appl. Phys.*, vol. 28, p. 1983, 1995.

[12] R. Barends, J. J. A. Baselmans, J. N. Hovenier, J. R. Gao, S. J. C. Yates, T. M. Klapwijk, and H. F. C. Hoevers, "Niobium and tantalum high-q resonators for photon detectors," *IEEE Trans. on Appl. Supercond.*, vol. 17, p. 263, 2007.

[13] J. Gao, M. Daal, A. Vayonakis, S. Kumar, J. Zmuidzinas, B. Sadoulet, B. A. Mazin, P. K. Day, and H. G. Leduc, "Experimental evidence for a surface distribution of two-level systems in superconducting lithographed microwave resonators," *Appl. Phys. Lett.*, vol. 92, p. 152505, 2008.

[14] R. D. Parks, *Superconductivity*, 1st ed. Marcel Dekker Inc. New York, 1969, vol. 2.

[15] F. C. Wellstood, C. Urbina, and J. Clarke, "Hot-electron effects in metals," *Phys. Rev. B*, vol. 49, p. 9, 1994.

[16] R. L. Kautz, G. Zimmerli, and J. M. Martinis, "Self-heating in the coulomb-blockade electrometer," *J. Appl. Phys.*, vol. 73, p. 2386, 1993.

[17] E. T. Swartz and P. O. Pohl, "Thermal boundary resistance," *Rev. Mod. Phys.*, vol. 61, p. 605, 1989.

[18] J. J. A. Baselmans, "Optimizing kinetic inductance detectors for low background applications," 2nd Workshop on the Physics and Applications of Superconducting Microresonators, June 19-20, 2008.